Published in final edited form as:
Bone. 2014 June ; 63: 29–35. doi:10.1016/j.bone.2014.02.012.

Type VII Collagen is Enriched in the Enamel Organic Matrix Associated with the Dentin-Enamel Junction of Mature Human Teeth

Jacob D. McGuire[1,*], **Mary P. Walker**[1,2], **Ahmad Mousa**[1], **Yong Wang**[1,2], and **Jeff P. Gorski**[1,2]

[1]Department of Oral and Craniofacial Sciences, School of Dentistry, University of Missouri-Kansas City, Kansas City, MO 64108

[2]Center of Excellence in Musculoskeletal and Dental Tissues, University of Missouri-Kansas City, Kansas City, MO 64108

Abstract

The inner enamel region of erupted teeth is known to exhibit higher fracture toughness and crack growth resistance than bulk phase enamel. However, an explanation for this behavior has been hampered by the lack of compositional information for the residual enamel organic matrix. Since enamel-forming ameloblasts are known to express type VII collagen and type VII collagen null mice display abnormal amelogenesis, the aim of this study was to determine whether type VII collagen is a component of the enamel organic matrix at the dentin-enamel junction (DEJ) of mature human teeth. Immunofluorescent confocal microscopy of demineralized tooth sections localized type VII collagen to the organic matrix surrounding individual enamel rods near the DEJ. Morphologically, immunoreactive type VII collagen helical-bundles resembled the gnarled-pattern of enamel rods detected by Coomassie Blue staining. Western blotting of whole crown or enamel matrix extracts also identified characteristic Mr=280 and 230 kDa type VII dimeric forms, which resolved into 75 and 25 kDa bands upon reduction. As expected, the collagenous domain of type VII collagen was resistant to pepsin digestion, but was susceptible to purified bacterial collagenase. These results demonstrate the inner enamel organic matrix in mature teeth contains macromolecular type VII collagen. Based on its physical association with the DEJ and its well-appreciated capacity to complex with other collagens, we hypothesize that enamel embedded type VII collagen fibrils may contribute not only to the structural resilience of enamel, but may also play a role in bonding enamel to dentin.

Please address all correspondence to: Dr. Jacob McGuire, Department of Oral and Craniofacial Sciences, School of Dentistry, Univ. of Missouri-Kansas City, 650 East 25th St., Room 3154, Kansas City, MO 64108, mcguireja@umkc.edu, Phone: 816-235-2179, Fax: 816-235-5524.

Keywords

Mature human enamel; Dentin-enamel junction; Type VII collagen; Immunofluorescent confocal microscopy

1. INTRODUCTION

The wear surface of mature teeth, enamel, is the most highly mineralized tissue in the body and is believed to be non-collagenous [1] and largely protein-free [2]. In contrast, the underlying dentin, which is similar to bone in composition [3], is a calcified, collagen-rich ectomesenchymal tissue that serves to support the outer, more brittle enamel [4]. The interfacial region coupling these dissimilar mineralized phases is known as the dentin-enamel junction (DEJ), which optically appears as an abrupt transition. However, a recent biomaterial study indicates the DEJ represents a broad functional zone that can, in part, be attributed to unidentified protein constituents at the dentin-enamel complex [5, 6]. Embryologically, the innermost enamel at the DEJ represents the position of the dental basement membrane [7, 8]. Composed largely of type IV/type VII collagen and laminin [9], these basement membrane constituents are widely believed to be removed by the time enamel secretion commences [10].

Although the extracellular organic matrix of enamel is largely removed, a small amount of protein remains in the inner region of the post-eruptive tissue [5]; distinct histologic features known as enamel tufts also extend vertically from the DEJ [11]. These hypomineralized fissures are believed to be a primary source of the fractures that develop in enamel during extensive function or overloading [12, 13]. The residual enamel organic matrix layer is believed to either represent organic ‘matter’ that fills cracks formed within enamel [13] or biological remnants that toughen the inner enamel region [6]. For example, alteration or removal of enamel’s residual organic matrix decreases its fracture toughness and resistance [14, 15]. By analogy, the material properties of mature bone are dependent upon the quality of its organic matrix [16]. Hampered by its insolubility [17], the molecular composition of the enamel organic matrix at the DEJ of mature teeth has remained a mystery for over fifty years [18].

Inactivating mutations in type VII collagen cause dystrophic forms of epidermolysis bullosa which manifest as skin fragility [19] and malformed enamel [20]. This phenotype is very similar to that exhibited by type VII collagen null mice [21]. Interestingly, type VII collagen is restricted to the basement membrane separating epithelial layers from their underlying stroma. In teeth, type VII collagen is localized to the epithelial mesenchymal junction during mouse enamel development [21] and the basement membrane of developing human tooth germs [22]. Additionally, type VII collagen is also known to be expressed by enamel-forming murine ameloblasts [21]. Based on type VII collagen’s requirement for anchoring the epidermis to the dermis in skin [23] and for normal amelogenesis [21], we sought to determine if type VII collagen is a component of the enamel organic matrix associated with the dentin-enamel junction of mature erupted teeth.

2. METHODS

2.1. Collection of Mature Teeth and Preparation

Mature erupted third molars without visual defect/caries, treatment planned for extraction, were acquired from local oral surgery clinics in the Kansas City area, according to a protocol approved by the University of Missouri Kansas City adult health science institutional review board (IRB#: 12-50-NHSR). Collected tooth specimens were washed using deionized water; and surface debris was removed using a scalpel and a stiff brush and stored at 4°C in 0.9% phosphate buffered saline (PBS) containing 0.002% sodium azide (NaN_3; Sigma-Aldrich, Saint Louis, MO) prior to processing. Following partial or complete root removal, the remaining crowns were processed in total or sectioned sagitally creating 500–1000 μm thick sections with a low-speed water cooled diamond saw (Isomet 1000, Buehler, Lake Bluff, IL).

2.2. Time-lapse Imaging of Enamel Demineralization and the Residual Enamel Matrix Layer

From three individual teeth, 500 μm sections were mounted in polymethyl methacrylate (Great Lakes Orthodontics, Tonawanda, New York). The sections were then immersed with the crown positioned down in 200 ml of 10% ethylenediaminetetraacetic acid (EDTA; Fischer Scientific, Hampton, NH) (pH 7.4), containing 0.002% NaN_3 and imaged under a fluorescent lamp with a Canon T2i digital SLR camera, and an EF 100 mm f/2.8 macro lens every 10 minutes for 120 hours, using a multi-function timer remote control.

2.3. Morphological Analysis of Enamel Tufts and the Enamel Matrix Layer

Similarly, 500 μm sections from six individual teeth, from different patients, were polished sequentially with 600 and 1200 grit silicon carbide paper concluding with 1-micron diamond polishing paste (Buehler). Sections were stained for 1 min in 0.2% (w/v) Coomassie Brilliant Blue R-250 (Sigma-Aldrich) in 50% methanol (Sigma-Aldrich) and 10% acetic acid (Sigma-Aldrich), destained and imaged for analysis of histologic enamel tufts. The same sections were then demineralized in 5% EDTA (pH 7.4) for 4 h followed by staining in Coomassie blue for 1 min, destained and re-imaged for the same analysis. A light microscope (Nikon Eclipse ME600, Melville, NY) equipped with a digital camera (Nikon DXM1200) was used to image sections.

2.4. Confocal Immunofluorescence Studies

Sections (~700 μm) from third molars from eight different patients were mounted on #1 chambered borosilicate coverglass (Lab-Tek, Rochester, NY) followed by complete demineralization in 10% EDTA (pH 7.4), containing 0.002% NaN_3 for 14 days.

Sections were then washed to remove residual EDTA with Buffer A [PBS (pH 7.4) containing 0.1% bovine serum albumin (BSA) and 0.05% Tween-20] and immediately blocked for 2 h in Buffer B [PBS (pH 7.4) containing 1% BSA and 0.05% Tween-20] and avidin D blocking solution (Vector Labs, Burlingame, CA). Sections were then incubated overnight at room temperature with primary antibody (1:200, catalog #234192, rabbit polyclonal anti-collagen type VII, Millipore, San Diego, CA) diluted in Buffer B and biotin

blocking solution (Vector Labs). Controls were treated with non-specific rabbit IgG (1:200, Sigma-Aldrich) under the same conditions.

For visualization, specimens were washed three times with Buffer A then incubated for 1 h with biotin conjugated-protein A (1:10,000, Millipore) in Buffer B; washed three times with Buffer A and then incubated with streptavidin labeled with AlexaFluor594 (1ug/ml, Jackson Laboratories, West Grove, PA) in Buffer B.

Serial z-focal plane images were captured on a confocal laser scanning microscope (CLSM; Leica TCS SP5 II, Wetzlar, Germany) at 405 and 594 nm using the resonant scanner and image formats of 1024 × 1024 pixels. Image J software was used to create z-stack and single plane images from the acquired data. Specific labeling was determined by subtracting the concomitant signal from the 594 and 405 channels using the same software.

2.5. Collagenase Treatment

Ten demineralized sections were treated with purified bacterial collagenase (0.075 mg/ml, catalog #C0773-3KV, Sigma-Aldrich) diluted in 50mM TES buffer (pH 7.4) containing 0.36 mM CaCl, for 6 h, and then immunolabeled and imaged as described above. Control sections were treated similarly with buffer alone.

2.6. Whole Crown and Enamel Protein Extraction

Extraction of proteins from whole tooth crowns from different patients was adapted from a protocol developed for extracting protein from bone [24]. Briefly, the roots were removed above the cementoenamel junction and the pulp tissue was extirpated and mechanically debrided. Each crown was flash-frozen in liquid nitrogen, pulverized, and mixed with extraction buffer containing 4 M guanidine hydrochloride, 0.5 M EDTA and a mixture of protease and phosphatase inhibitors for 72 hours at 4°C. Samples were then centrifuged and the supernatant was dialyzed three times each against water and then against 5% acetic acid at 4°C using 6–8 kDa molecular weight cut-off dialysis tubing (Spectrum Laboratories, Rancho Dominguez, CA). Extracts were lyophilized and stored at −80°C. Protein amounts were determined colorimetrically using the NI™ (Non-Interfering™)Protein Assay kit (G-Biosciences, Saint Louis, MO).

Extraction of enamel matrix proteins from six tooth crowns was accomplished by demineralizing whole crowns, enamel side up, in 40 ml of 10% EDTA (7.4 pH) containing 0.002% NaN_3 for 14 days at 20°C. The residual enamel matrix layer was gently debrided from the dentin surface with a soft applicator brush (displayed in Fig. 1e), followed by removal of the intact, underlying dentin. Extracts were then dialyzed, lyophilized, stored, and protein amounts determined as described above.

2.7. Pepsin Digestion

Extracted enamel matrix protein fractions from two tooth crowns were incubated separately with pepsin using a well-established protocol [25]. Protein weight after lyophilization was determined directly and each enamel sample was rehydrated at 1 mg/ml in 0.5 M acetic acid (Sigma-Aldrich). The specimens were then incubated with pepsin (100 μg/ml, Millipore) at

4°C for 48 hours. Additional enamel matrix fractions from each specimen were incubated similarly without pepsin (negative controls). Digestion reactions were inactivated by heat, lyophilized and stored frozen prior to analysis.

2.8. SDS-PAGE and immunoblotting

Pepsin digested and control protein extracts from whole crowns and enamel matrixes were dissociated in SDS/8M urea sample buffer, heated at 95°C, and electrophoresed as previously described using 4–20% linear gradient and 7.5% gels [26]. Blots were incubated with either primary mouse anti-type VII collagen monoclonal antibody recognizing the non-helical carboxy terminal region of the collagen VII dimer (1:500, clone LH7.2, Sigma-Aldrich) or primary rabbit anti-type VII polyclonal antibody (1:500, catalog #234192, Millipore), and then subsequently with horseradish peroxidase-conjugated goat-anti-mouse or goat-anti-rabbit IgG (1:10,000, BioRad, Irvine, CA) secondary antibodies, respectively. Chemiluminescent digital images were captured with a Fuji LAS-4000 imager (GE, Piscataway, NJ).

3. RESULTS

3.1. Demineralization of Mature Teeth Uncovers an Enamel Protein Matrix Layer at the Dentin Surface

Time lapse observation during demineralization revealed a novel enamel organic matrix layer adjacent to the dentinal surface (Fig. 1a–f). In all specimens, the enamel matrix appeared as a layer homogenously distributed across the dentinal surface (Fig. 1d). The matrix layer was easily detached and removed from the dentin with a brush following dissolution of the surrounding mineral phase (Fig. 1e–f). The greatest amount of the organic layer was observed in the cuspal/occlusal region (Fig. 1d–e). We believe this enamel matrix layer is identical to the 150–300 μm wide organic layer observed previously by SEM and by confocal Raman spectroscopy [5].

3.2. Enamel Tuft Structures are Associated with the Enamel Organic Matrix

Coomassie Brilliant Blue staining of tooth sections demonstrated the appearance of enamel ‘tufts’ (Fig. 2a, black arrow). Interestingly, the distribution of the ‘tuft’ fissures correlates with some features of the enamel organic matrix layer visualized after demineralization (Fig. 2b). Specifically, both structures arise, are congruent, and extend coronally from the DEJ, with the tufts being observed within the organic matrix layer, which appears white in undemineralized sections (Fig. 2a). The height of the tuft projections coincided with the thickness of the matrix layer. However, a careful analysis indicates the rather monolithic enamel tuft extensions are distinct from blue stained, spiral-shaped bundles composing the organic matrix layer (Fig. 2b, white arrow). Importantly, the helical corkscrew pattern of enamel matrix bundles in their longitudinal dimension (Figs. 2b) corresponds with gnarled enamel associated with twisting enamel rods in the cuspal regions [27]. When Figures 2a and 2b are overlaid, the enamel tuft projections do not superimpose with the spiral strands of the surrounding organic matrix layer (Fig. 2c). In each specimen, enamel tufts and the matrix layer were most prominent in the coronal/occlusal regions, which are exposed to masticatory compressive forces in vivo (Fig. 2a and b). In contrast, in cervical regions

subject predominantly to flexural forces, the organic matrix was thin and tufts were largely absent (Fig. 2d–f).

3.3. Confocal Microscopy Reveals Fibrillar Sheets of Type VII Collagen in the Enamel Organic Matrix

To investigate whether type VII collagen is present in mature teeth, we carried out immunofluorescent staining on human tooth crown sections containing enamel, the dentin-enamel junction, and dentin. In order to expose epitopes, crown sections were first decalcified at room temperature. While non-immune controls were negative (Fig 3a and b, respectively), anti-type VII collagen antibodies specifically labeled multi-stranded, fibrillar arrays that originated within the DEJ and extended into the enamel (Fig. 3c). These fibrillar arrays were observed in predominantly cuspal/occlusal regions, projecting coronally 200–400 μm into enamel, and were spaced 100–200 μm along the DEJ (Fig. 3c). Type VII collagen positive fibrillar bundles exhibited a wavy pattern (Fig. 3 c, e, f), which mimicked structures observed in Coomassie Blue stained sections (Fig. 2b). Moreover, cross-sectional views show that type VII collagen is part of the tubular protein sheath surrounding individual enamel rods (Fig. 3g). Technical difficulties prevented similar analyses of sections from the cervical region (not shown).

3.4. Type VII Collagen Within the Enamel Matrix is Susceptible to Bacterial Collagenase

Confirmation of the collagenous character of immunostained fibrillar arrays was obtained by incubation of crown sections with purified bacterial collagenase, which cleaves glycine-X bonds in collagenous domains including that for type VII collagen [28]. As shown in Figure 4b, bacterial collagenase-treated sections exhibited a much attenuated and fragmented staining pattern. In contrast, the pattern of immunostaining for digestion controls was unchanged (Fig. 4a).

3.5. Western Blotting Confirms the Presence of Type VII Collagen in Enamel

To confirm the presence of type VII collagen, eight individual crown extracts and enamel matrix protein preparations from four individual molars from patients ranging from 18–73 years old were subjected to immunoblotting. Under reduced conditions, SDS-PAGE results show an enrichment of 75 and 25 kDa type VII collagen fragments using monoclonal (Fig. 5a, c) or polyclonal (Fig. 5b, d) anti-type VII collagen antibodies. Similar molecular weight fragments were also demonstrated in enamel matrix protein preparations with a third monospecific antitype VII collagen antibody (results not shown). Figure 5e shows that unreduced type VII immunoreactive bands migrated as a disulfide-bonded dimer at 280 and 230 kDa (lanes 1 and 2). After reduction, this dimer dissociated into its 75 kDa monomer form (lanes 1R and 2R), which was resistant to pepsin digestion (Fig. 5f).

4. DISCUSSION

In contrast to dentin, mature enamel is believed to be devoid of an organic matrix [4] due to its low content of organic compounds by weight (~1%) [2]. However, Eastoe [18], Sognnaes [29], and Weatherell et al. [11] showed that human enamel does contain a highly insoluble fibrillar proteinaceous component, which we believe represents the enamel organic matrix

observed in the time lapse images after complete demineralization, and the 150–300 μm wide organic layer observed previously by SEM and Raman spectroscopy [5]. Re-evaluation of these early studies reveals several shared chemical and physical features with type VII collagen. For example, the twisted corkscrew shape and cysteine content of enamel "ribbons" identified by these authors closely resemble type VII collagen fibrillar bundles [30] shown here to emanate from the DEJ. Enamel is thought to be collagen-free based on the virtual absence of hydroxyproline and hydroxylysine in the mature tissue [1, 2]. However, this estimate assumes a uniform distribution within the enamel phase. In this way, local enrichment of type VII collagen observed here within the enamel organic matrix adjacent to the DEJ would be consistent with the low, but apparently real levels of hydroxyproline detected in mature enamel [31, 32].

Immunofluorescent images show that type VII collagen is distributed within the enamel matrix layer in a pattern reflecting the underlying enamel rod architecture. Importantly, cuspal regions morphologically contain more of the enamel organic matrix. Yet its distribution as large 200–400 μm macromolecular extensions contrasts with other epithelial-derived tissues where it is restricted to the sub-basal laminae of the basement membrane [33]. Despite these morphological differences, our identification of type VII collagen is also supported by separate western blotting results and by its differential susceptibility to purified bacterial collagenase and pepsin.

The unique helical pattern of type VII collagen within the enamel organic matrix as compared to other epithelial tissues cannot be fully explained at present. However, the hydrodynamic sizes of the immunoreactive dimers of M_r= 280–230 kDa observed in enamel matrix extracts is similar to that of intact skin-derived type VII collagen [34, 35]. As expected for type VII collagen under reducing conditions, the dimer separated into a 75 kDa monomer that was pepsin resistant [33]; and an amino-terminal 25 kDa fragment (35). These results suggest that disulfide bonding may contribute to the well-known insolubility of the enamel organic matrix [17], and why it may be protected during matrix degradation, facilitating its retention after amelogenesis. Furthermore, the self-healing capacity of enamel in the DEJ region described by Myoung et al. [13] could be related to the cross-linking capacity of type VII collagen [33].

The well-known fracture resistance and damage tolerant properties of cuspal enamel remain to be fully explained [12, 36]. For example, the path of experimentally induced cracks was blunted upon reaching a 50–150 μm wide region of inner enamel adjacent to the DEJ that displayed material properties [37–39] distinct from outer enamel. Because the contribution of the mineral phase to enamel's mechanical properties dominates current views, residual enamel matrix proteins are considered biological contaminants [6], or degradation products that do not play a major structural role [27]. In contrast, the present study indicates that the inner enamel region contains macromolecular type VII collagen that is recoverable as a separate insoluble matrix when the surrounding mineral is removed. It's preferential localization and distribution to hydroxyapatite prism/rod sheaths of undulating bundles of cuspal/occlusal enamel, as opposed to cervical enamel (which is prismless) raises several questions. Since cuspal/occlusal enamel is subjected primarily to compressive forces during mastication, we speculate that the parallel orientation of type VII collagen fibrillar bundles

along the expected lines of applied force may imply a stabilizing role in reducing stress between the enamel and dentin layers. This stress relieving property could also reduce occlusal stresses, inhibiting catastrophic crack growth within enamel [40]. Protein-protein interactions between type VII collagen and other components of the basement membrane separating the epidermal and dermal layers are responsible for maintaining the integrity of skin [41]. Although occlusal functional force can produce a combination of compressive, tensile, flexure, and shear stresses, teeth, like skin, do not typically separate into the two layers. Mutations in type VII collagen lead to abnormal amelogenesis and abnormal enamel rod orientation, which can be completely rescued by restoration of expression [21]. However, the functional impact of this altered rod orientation has not been carefully evaluated.

In summary, we propose that identification of type VII collagen may help to explain the unusual fracture resistance and toughness of the inner enamel adjacent to the dentin-enamel junction of mature teeth. In this regard, it will be important in the future to probe for other basement membrane proteins that may be present within the DEJ, and to test the tooth material wear and fracture resistant properties of type VII collagen null and rescued mice. Similarly, deficiency of type VII collagen is associated with epidermolysis bullosa dystrophica [42] that is associated with a number of oral complications including enamel hypoplasia and rapid attrition of the teeth [43]. In support of our functional hypothesis for type VII collagen, enamel hypoplasia presents as an abnormally thin enamel layer, which exhibits rapid attrition under normal mechanical forces from opposing teeth. Since pathologic delamination of enamel from the underlying dentin occurs in patients after high dose oral cancer radiotherapy, future studies will also investigate whether radiation causes loss or degradation of enamel type VII collagen.

5. CONCLUSIONS

We have identified for the first time that type VII collagen is a collagenase sensitive, pepsin resistant component of the enamel organic matrix layer of mature human tooth enamel. Type VII collagen extends as large macromolecular fibrillar bundles from the DEJ towards the outer enamel surface, and is preferentially localized to the outer protein sheaths of hydroxyapatite rods. Since type VII collagen acts as an anchoring fibril in the basement membrane of other epithelial tissues, we speculate that it may play a similar role at the DEJ serving to mechanically stabilize the enamel and dentin interface.

Acknowledgments

This study was supported by NIH/NIDCR grants R01-DE021462 and F32-DE022984. The authors wish to thank Ms. Rachel Reed, Dr. Steven Thomas, Dr. Erica Perryn, and Dr. LeAnn Tiede-Lewis for their excellent technical assistance. In addition, we acknowledge use of the confocal microscope in the University Missouri, Kansas City School of Dentistry Confocal Microscopy Core. This facility is supported by the UMKC Office of Research Services, UMKC Center of Excellence in Dental and Musculoskeletal Tissues and NIH grant S10RR027668.

References

1. Fincham A, Moradian-Oldak J, Simmer J. The structural biology of the developing dental enamel matrix. J Struct Biol. 1999; 126:270–299. [PubMed: 10441532]
2. Schroeder, HE. Oral Structural Biology. Stuttgart, Germany: Georg Thieme Verlag; 1991.

3. Opsahl Vital S, Gaucher C, Bardet C, Rowe PS, George A, Linglart A, Chaussain C. Tooth dentin defects reflect genetic disorders affecting bone mineralization. Bone. 2012; 50:989–997. [PubMed: 22296718]
4. Simmer J, Hu J-C. Dental enamel formation and its impact on clinical dentistry. J Dent Educ. 2001; 65:896–905. [PubMed: 11569606]
5. Dusevich V, Xu C, Wang Y, Walker M, Gorski J. Identification of a protein-containing enamel matrix layer which bridges with the dentine–enamel junction of adult human teeth. Arch Oral Biol. 2012; 57:1585–1594. [PubMed: 22609172]
6. White SN, Paine ML, Luo W, Sarikaya M, Fong H, Yu Z, Li ZC, Snead ML. The dentino- enamel junction is a broad transitional zone uniting dissimilar bioceramic composites. J Am Ceram Soc. 2000; 83:238–240.
7. Paine M, White S, Luo W, Fong H, Sarikaya M, Snead M. Regulated gene expression dictates enamel structure and tooth function. Matrix Biol. 2001; 20:273–292. [PubMed: 11566262]
8. Slavkin HC, Brownell AG, Bringas P Jr, MacDougall M, Bessem C. Basal lamina persistence during epithelial-mesenchymal interactions in murine tooth development in vitro. J Craniofac Genet Dev Biol. 1983; 3:387–407. [PubMed: 6662909]
9. Timpl R. Structure and biological activity of basement membrane proteins. Eur J Biochem. 1989; 180:487–502. [PubMed: 2653817]
10. Heikinheimo K, Salo T. Expression of basement membrane type IV collagen and type IV collagenases (MMP-2 and MMP-9) in human fetal teeth. J Dent Res. 1995; 74:1226–34. [PubMed: 7790601]
11. Weatherell J, Weidmann S, Eyre D. Histological appearance and chemical composition of enamel protein from mature human molars. Caries Res. 1968; 2:281–193. [PubMed: 4924678]
12. Chai H, Lee J, Constantino P, Lucas P, Lawn B. Remarkable resilience of teeth. Proceedings of the National Academy of Sciences of the United States of America. 2009; 106:7289–7293. [PubMed: 19365079]
13. Myoung S, Lee J, Constantino P, Lucas P, Chai H, Lawn B. Morphology and fracture of enamel. J Biomech. 2009; 42:1947–1951. [PubMed: 19559438]
14. Seghi RR, Denry J. Effects of external bleaching on indentation and abrasion characteristics of human enamel in vitro. J Dent Res. 1992; 71:1340–1344. [PubMed: 1613185]
15. Baldassarri M, Margolis HC, Beniash E. Compositional determinants of mechanical properties of enamel. J Dent Res. 2008; 87:645–649. [PubMed: 18573984]
16. Burr DB. The contribution of the organic matrix to bone's material properties. Bone. 2002; 31:8–11. [PubMed: 12110405]
17. Robinson C, Hudson J. Tuft protein: protein cross-linking in enamel development. Eur J Oral Sci. 2011; 119:50–54. [PubMed: 22243226]
18. Eastoe J. Organic matrix of tooth enamel. Nature. 1960; 197:411–412. [PubMed: 13819116]
19. Christiano A, Greenspan D, Hoffman G, Zhang X, Tamai Y, Lin A, Dietz H, Hovnanian A, Uitto J. A missense mutation in type VII collagen in two affected siblings with recessive dystrophic epidermolysis bullosa. Nat Genet. 1993; 4:62–66. [PubMed: 8513326]
20. Wright J. Oral manifestations in the epidermoysis bullosa spectrum. Dermatol Clin. 2010; 28:159–164. [PubMed: 19945630]
21. Umemoto H, Akiyama M, Domon T, Nomura T, Shinkuma S, Ito K, Asaka T, Sawamura D, Uitto J, Uo M, Kitagawa Y, Shimizu H. Type VII collagen deficiency causes defective tooth enamel formation due to poor differentiation of ameloblasts. Am J Pathol. 2012; 181:1659–1671. [PubMed: 22940071]
22. Heikinheimo K, Morgan PR, Happonen R-P, Stenman G, Virtanen I. Distribution of extracellular matrix proteins in odontogenic tumours and developing teeth. Vircows Archiv B Cell Pathol. 1991; 61:101–109.
23. Villone D, Fritsch A, Koch M, Bruckner-Tuderman L, Hansen U, Brucker P. Supramolecular interactions in the dermo-epidermal junction zone: Anchoring fibril- collagen VII tightly binds to banded collagen fibrils. J Biol Chem. 2008; 283:24506–13. [PubMed: 18599485]

24. Gorski JP, Kremer EA, Chen Y, Ryan S, Fullenkamp C, Delviscio J, Jensen K, McKee MD. Bone acidic glycoprotein-75 self-associates to form macromolecular complexes in vitro and in vivo with the potential to sequester phosphate ions. J Cell Biochem. 1997; 64:547–64. [PubMed: 9093904]
25. Bentz H, Morris NP, Murray LW, Sakai LY, Hollister DW, Burgeson RE. Isolation and partial characterization of a new human collagen with an extended triple-helical structural domain. Proc Natl Acad Sci USA. 1983; 80:3168–72. [PubMed: 6574478]
26. Gorski JP, Huffman NT, Chittur S, Midura RJ, Black C, Oxford J, Seidah NG. Inhibition of proprotein convertase SKI-1 blocks transcription of key extracellular matrix genes regulating osteoblastic mineralization. J Biol Chem. 2011; 286:1836–49. [PubMed: 21075843]
27. Nanci, A. Ten Cate's oral histology: development, structure, and function. 7. St. Louis: Mosby, Inc; 2008.
28. Lapiere J, Woodley D, Parente M, Iwasaki T, Wynn K, Christiano A, Uitoo J. Epitope mapping of type VII collagen. Identification of discrete peptide sequences recognized by sera from patients with acquired epidermolysis bullosa. J Clin Invest. 1993; 92:1831–1839. [PubMed: 7691888]
29. Sognnaes RF. The Organic Elements of the Enamel: II. the Organic Framework of the Internal Part of the Enamel. with Special Regard to the Organic Basis for the So-Called Tufts and Schreger's. Bands J Dent Res. 1949; 28:549.
30. Lunstrum G, Sakai L, Keene D, Morris N, Burgeson R. Large complex globular domains of type VII procollagen contribute to the structure of anchoring fibrils. J Biol Chem. 1986; 19:9042–9048. [PubMed: 3013874]
31. Acil Y, Mobasseri AE, Warnke PH, Terheyden H, Wiltfang J, Springer I. Detection of mature collagen in human dental enamel. Calcif Tissue Int. 2005; 76:121–126. [PubMed: 15558350]
32. Burrows, LR. An investigation of proteins of human enamel matrix with special reference to the amino acid hydroxyproline. In: Stack, MV.; Fearnhead, RW., editors. Proceedings of an International symposium on the composition, properties, and fundamental structure of tooth enamel. John Wright & Sons Ltd; 1964. p. 59-62.
33. Morris NP, Keene DR, Glanville R, Bentz H, Burgeson RE. The tissue form of type VII collagen is an antiparallel dimer. J Biol Chem. 1986; 261:5638–44. [PubMed: 3082888]
34. Bruckner-Tuderman L, Schnyder UW, Winterhalter KH, Bruckner P. Tissue form of type VII collagen from human skin and dermal fibroblasts in culture. Eur J Biochem. 1987; 165:607–611. [PubMed: 3109908]
35. Woodley DT, Burgeson RE, Lunstrum G, Bruckner-Tuderman L, Reese MJ, Briggaman RA. Epidermolysis bullosa acquisita antigen is a globular carboxyl terminus of type VII procollagen. J Clin Invest. 1988; 81:683–687. [PubMed: 3278005]
36. Lawn B, Lee J. Analysis of fracture and deformation modes in teeth subjected to occlusal loading. Acta Biomater. 2009; 5:2213–2221. [PubMed: 19268644]
37. Lin C, Douglas W. Structure-property relations and crack resistance at the bovine dentin- enamel junction. J Dent Res. 1994; 73:1072–1078. [PubMed: 8006234]
38. Dong X, Ruse N. Fatigue crack propagation path across the dentinoenamel junction complex in human teeth. J Biomed Mater Res. 2003; 66A:103–109.
39. Bechtle S, Fett T, Rizzi G, Habelitz S, Klocke A, Schneider G. Crack arrest within teeth at the dentinoenamel junction caused by elastic modulus mismatch. Biomaterials. 2010; 31:4238–4247. [PubMed: 20167362]
40. White SN, Luo W, Paine ML, Fong H, Sarikaya M, Snead M. Biological organization of hydroxyapatite crystallites into a fibrous continuum toughens and controls anisotropy in human enamel. J Dent Res. 2001; 80:321–326. [PubMed: 11269723]
41. Burgeson R, Christiano A. The dermal—epidermal junction. Curr Opin Cell Biol. 1997; 9:651–658. [PubMed: 9330868]
42. Bart B, Gorlin R, Anderson V, Lynch F. Congential localized absence of skin and associated abnormalities resembling epidermolysis bullosa: a new syndrome. Arch Dermatol. 1966; 93:296–304. [PubMed: 5910871]
43. Wiebe C, Larjava H. Do mutations in the basement membrane zone affect the human periodontium? Review with special reference to epidermolysis bullosa. J West Soc Periodontal Periodontal Abstr. 1998; 46:5–18. [PubMed: 9709672]

HIGHLIGHTS

1. Macromolecular type VII collagen was identified for the first time in the organic matrix layer of mature enamel.
2. Type VII collagen was identified via its immunoreactivity with multiple antibodies, sensitivity to purified collagenase, and resistance to pepsin.
3. Morphologically, type VII collagen exhibits an unusual corkscrew distribution pattern relative to the dentin enamel interface.
4. Type VII collagen is preferentially localized to the proteinaceous outer rod sheath of hydroxyapatite enamel rods.
5. Type VII collagen may function as part of an anchoring complex which mechanically stabilizes the enamel layer.

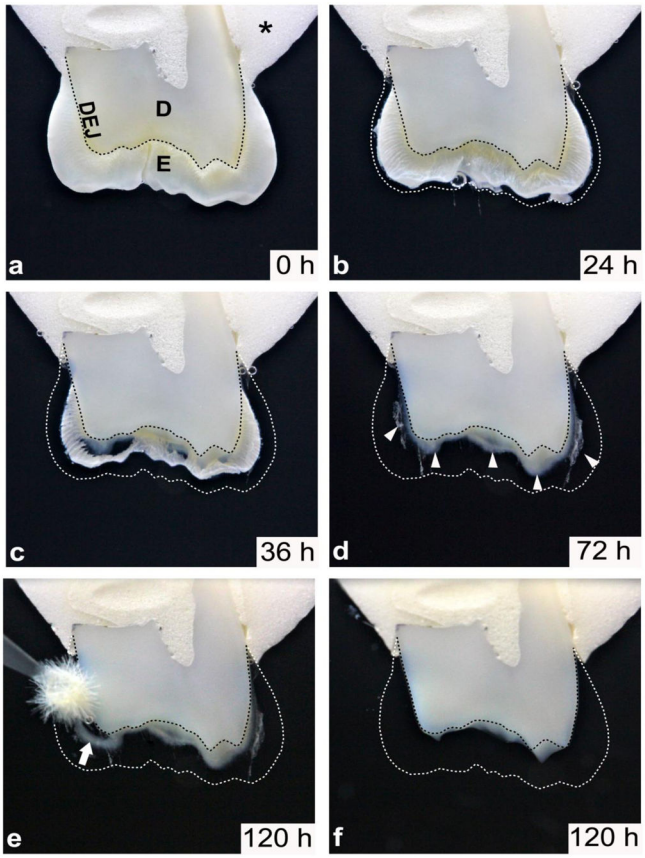

Figure 1. Enamel organic matrix resides within the inner layer of enamel and is congruent with underlying dentin

Time lapse imaging of a demineralizing crown section captured over a 120 hour period as described in METHODS. **a)** Acrylic embedded (asterick) upper molar crown section, immersed in neutral 10% EDTA, displays the enamel and dentin layers joining at the optical DEJ (dotted black line). **b)** The same section after 24 hours and **c)** 36 hours of demineralization reveals the progression of enamel demineralization, noted by the original coronal position of the enamel (dotted white line). **d)** Following 72 hours of demineralization, the residual organic matrix is seen within the inner layer of enamel distributed along the dentin, predominantly in the cuspal regions (white arrowheads). **e)** The enamel is completely demineralized after 120 hours and the enamel organic matrix is easily detached from the dentinal surface with a soft applicator brush (white arrow). **f)** Following gentle removal of the organic matrix as shown in **e)**, the underlying dentin outline is unchanged, as noted by the optical DEJ (dotted black line). **KEY: ***, acrylic; **E**, enamel; **D**, dentin; **DEJ**, dentin-enamel junction (dotted black line), enamel outline (dotted white line).

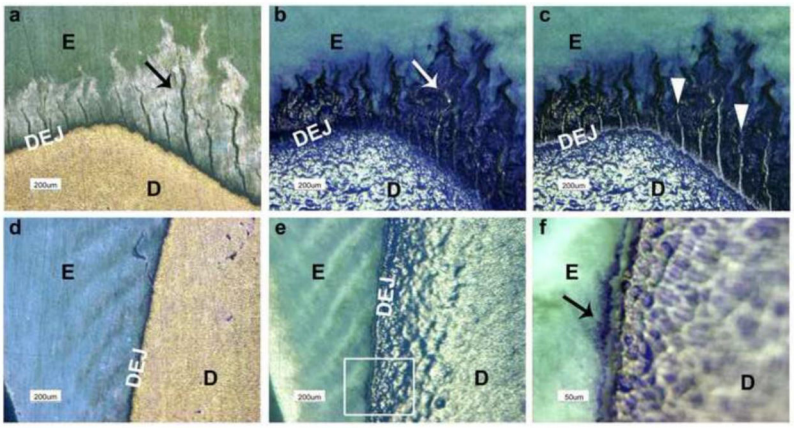

Figure 2. Enamel organic matrix is composed of spiral shaped bundles which are distinct from histologic enamel tuft projections

a) Enamel tufts are observed in undemineralized human molar crown section after staining with Coomassie blue. Histologic enamel tufts (black arrow) of differing lengths are orientated in a coronal direction and emanate from the DEJ. The outline of the organic matrix layer surrounding the enamel tufts can be seen due to light etching by the acetic acid in the stain. **b)** The same section depicted in **a)** was then demineralized for 4 h and then restained. The organic matrix layer, congruent with and emanating from the DEJ, is now composed of blue stained, corkscrew shaped parallel bundles and is enriched in the cuspal/occlusal region. Enamel tufts were found to be distinct from the blue stained fibrillar bundles (white arrow). **c)** An overlay of enamel tufts (white arrowheads) taken from **a)** onto the organic matrix layer in **b)** confirms the distinct morphologic patterns of these two structures arising from the DEJ. **d)** Microscopic field showing a cervical region of the same Coomassie blue stained tooth crown section prior to demineralization. **e)** The same cervical region shown in **d)** after 4 h of demineralization and restaining. The enamel matrix layer was thin along the DEJ and enamel tufts were largely absent. **f)** An enlarged view of the white box in **e)** illustrating the thin organic matrix (black arrow) at the DEJ. Notably, deeper staining of dentin requires a longer staining interval. **KEY: E**, enamel; **D**, dentin; and **DEJ**, dentin-enamel junction

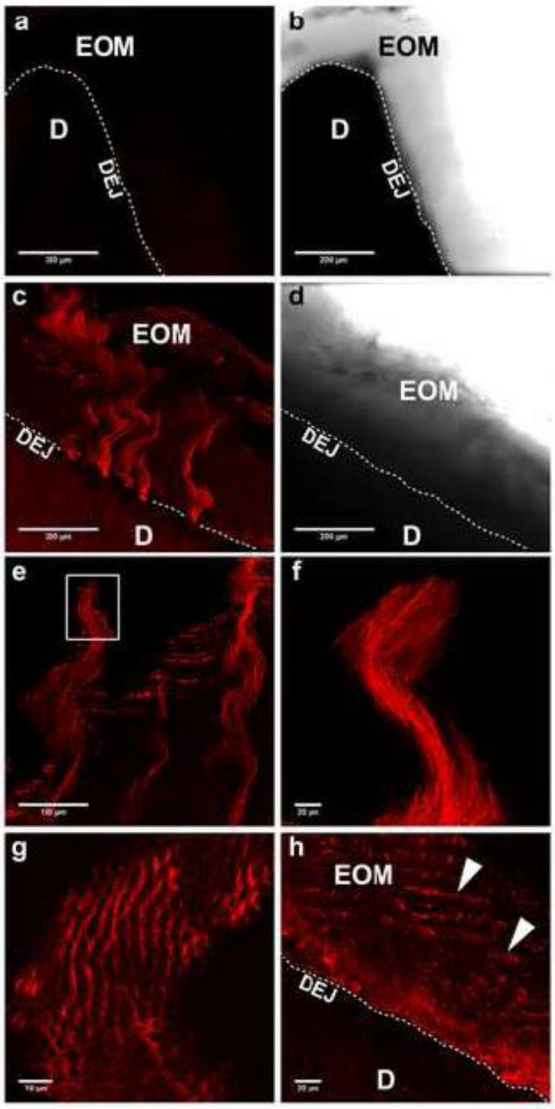

Figure 3. Type VII collagen Immunoreactive spiral shaped fibrillar bundles emanate from the DEJ and project coronally up to 400 μm into the enamel

Immunofluourescently stained images were obtained using confocal microscopy as described in METHODS. Results shown are representative of eight individual teeth. **a)** Control section stained with non-immune rabbit IgG showed minimal staining. **b)** Respective bright field image of microscopic field in **a**) which shows the position of the enamel organic matrix along the dentin after complete demineralization. **c)** Lower power view of fibrillar arrays of type VII collagen emanating from the DEJ and projecting coronally. **d)** Paired bright field image of **c). e)** A higher power view of spiral shaped type VII collagen bundles near the coronal limit of the enamel organic matrix. **f)** Enlarged view of the white box in **e). g)** Cross-sectional view of the coronal end of a type VII collagen fibrillar bundle demonstrating its “fish-scale” structure and relationship with the tubular sheath surrounding the enamel rods. **h)** On some sections, the type VII collagen immunostaining pattern appeared as parallel corrugated rows (arrowheads) within the organic matrix. **KEY: EOM**, enamel organic matrix; **D**, dentin; **DEJ**, dentin-enamel junction (dotted white line).

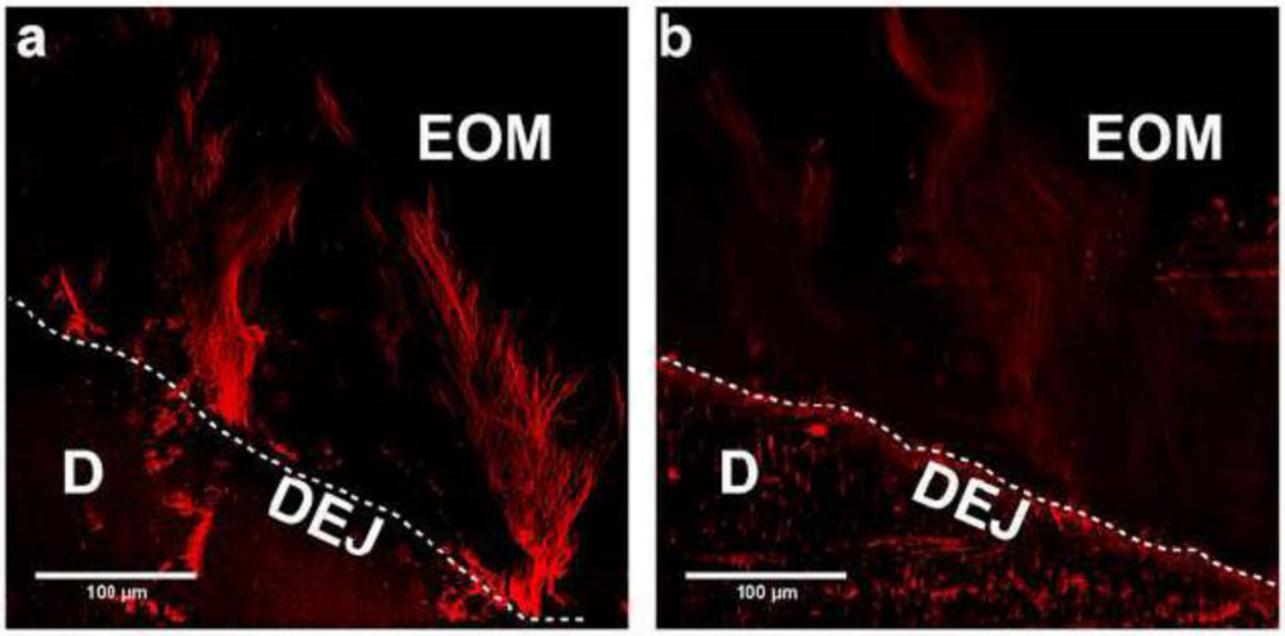

Figure 4. Immunostained type VII collagen fibrillar bundles within the enamel organic matrix are susceptible to bacterial collagenase degradation

Immunofluourescently stained images were obtained using confocal microscopy as described in METHODS. Results shown are representative of four experiments. **a)** Immunostained appearance of digestion control section without collagenase. **b)** Immunoreactivity of type VII collagen fibrillar bundles was greatly diminished after 6 h digestion with purified collagenase. **KEY: EOM**, enamel organic matrix; **D**, dentin; and **DEJ**, dentin-enamel junction (dotted white line).

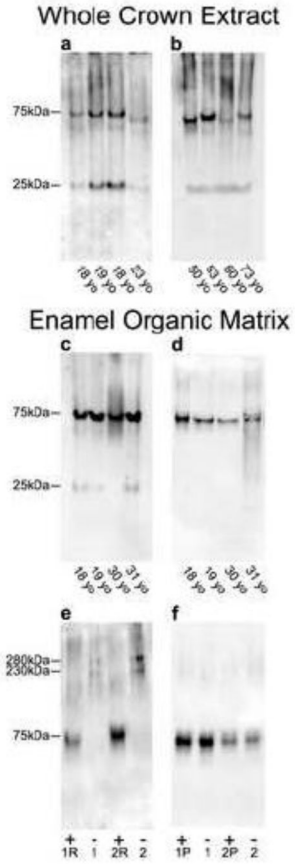

Figure 5. Immunostaining of whole crown extracts and enamel organic matrix fraction demonstrates an enrichment of type VII collagen and associated fragments

a–d) Protein extracts from whole tooth crowns and the enamel organic matrix (see METHODS) were electrophoresed under reducing conditions using 4–20% linear gradient gels and electroblotted onto polyvinylidene difluoride membranes and immunostained with a monoclonal (**a and c**) or polyclonal (**b and d**) anti-type VII collagen antibodies. **a–b)** Type VII collagen fragments with Mr=75 kDa and 25 kDa were enriched in whole crown extracts. **c–d)** Enamel extracts containing only the enamel organic matrix fraction displayed an enrichment of similar type VII collagen-derived fragments, localizing type VII collagen to the enamel. Importantly, immunolabeling was not dependent on patient age and was similar with both antibodies. **e–f)** Organic matrix proteins electrophoresed using 7.5% gels and electroblotted onto polyvinylidene difluoride membranes and immunostained with a polyclonal anti-type VII collagen antibody. **e)** Enamel matrix fraction from two individual molars was electrophoresed either reduced (1R and 2R) or non-reduced (1 and 2). Non-reduced samples displayed higher molecular weight mobilities of 280 and 230 kDa, which shifted to Mr=75 kDa fragment after reduction. **f)** Analysis of enamel matrix fraction treated with or without pepsin digestion, followed by reduction, showed that the Mr=75 kDa type VII collagen fragment is pepsin resistant and likely represents a collagenous domain fragment. The amount of protein loaded onto gel lanes for blots **a–b** was 15 μg and for blots **c–f** was 30 μg. Antibodies used were: monoclonal anti-type VII collagen antibody (LH7.2) which recognizes the non-helical carboxy terminal region of the collagen dimer; and, polyclonal anti-type VII collagen antibody. Molecular weight estimates are based on globular standards co-electrophoresed on the same gel.